P.V. GALIY,[1] YA.B. LOSOVYJ,[2] T.M. NENCHUK,[1] I.R. YAROVETS'[1]

[1] Ivan Franko National University of Lviv, Faculty of Electronics,
Department for Semiconductors Physics
(50, Dragomanov Str., Lviv 79005, Ukraine; e-mail: galiy@electronics.lnu.edu.ua)
[2] Nanoscale Characterization Facility, Department of Chemistry, Indiana University
(800, E. Kirkwood Ave., Bloomington, IN 47405, USA)

LOW-ENERGY-ELECTRON-DIFFRACTION STRUCTURAL STUDIES OF (100) CLEAVAGE SURFACES OF In_4Se_3 LAYERED CRYSTALS

PACS 61.14.Hg, 68.47.Fg, 68.60.Dv

Structure stability and "thermal" parameters of (100) cleavage surfaces of In_4Se_3 crystals have been studied using the low energy electron diffraction method. The structure of (100) cleavage surfaces of In_4Se_3 crystals is shown to be stable and not subjected to any reconstruction in a wide temperature interval of 77–295 K. The Debye temperature and the Debye–Waller factor of studied surfaces were calculated on the basis of experimental data obtained for the temperature dependence of the intensities of diffraction spots (the intensities decreased, as the temperature grew). It is confirmed that the Debye temperatures for the cleavage surface (100) and in the bulk of In_4Se_3 crystal are different. The anisotropy of thermal expansion along the main crystallographic lattice directions in the cleavage plane (100) of In_4Se_3 is established.

Keywords: low energy electron diffraction, layered crystals, interlayer cleavage surfaces, Debye temperature, Debye–Waller factor, anisotropy of thermal expansion.

1. Introduction

For plenty of compounds, the surface of their solid phase regarded as an interface is known to possess many properties different from the bulk ones: it has its own crystallography, electron energy structure, electron and phonon spectra, and thermodynamic (thermal) characteristics [1–4]. The surface of solids is associated with numerous atomic processes such as the adsorption and the desorption of atoms and molecules, dissociation of molecules, migration of atoms on the surface, their diffusion into the solid bulk, reactions on the surface, and others [1–4]. Nowadays, the level of comprehension of those and many other surface phenomena determines the progress in such important domains of science and technology as, e.g., thin-film micro- and nanoelectronics, catalysis, nanotechnology, and nanoengineering.

Among the methods aimed at studying the surface of semiconductor electronic materials, the highly informative methods of electron spectroscopy dominate. The microscopic characteristics of the surface—besides the element and phase compositions, and the electron energy structure—also include the geometry of atomic arrangement on the surface (the atomic structure or the surface crystallography) and the dynamics of atoms or the phonon spectra of a surface, which determine its thermal properties.

Low-energy electron diffraction (LEED) [1–4] is one of the methods of electron spectroscopy of the surface that enables the direct information concerning the surface crystallography to be obtained. Using LEED, it is possible to determine two-dimensional structures on the surface and their parameters, detect the reconstruction of both the surface itself and monolayer structures formed on it, and so on.

Layered crystals In_4Se_3 with a strong covalent-ionic interaction in the layer and the weak van der Waals coupling between the layers [5], as well as their cleavage surfaces (CSs) (100), are objects of modern researches [6–8], which provide a new understanding of the properties of low-dimensional (2D) and chain-like structures and their probable technological application [9]. The weak van der Waals coupling between the layers allows one to easily obtain *in situ* the interlayer CSs (100) of In_4Se_3 (Fig. 1, panels *a* and *b*) almost free of "broken" and unsaturated electron bonds [10].

In particular, according to the results obtained by us in works [6–8] using the methods of atomic force (AFM) and scanning tunnel (STM) microscopies, the CSs (100) obtained for In_4Se_3 under ultrahigh vacuum (UHV) of the pressure $P = 1.5 \times \times 10^{10}$ Torr were structurally stable and characterized by a groove, chain-like structure (Fig. 1, *c*). They can be used as anisotropic, weakly conducting matrices/patterns/substrates for the creation of surface conducting (In/Au) nanowires or other nanostructures.

Researches of CSs obtained under UHV for MoS_2, WSe_2, SnS_2 [11], and GaSe [12] cleavage surfaces using the methods of LEED, STM, and ultra-violet photoelectron spectroscopy [9] testify to the absence of hexagonal systems of unsaturated electron bonds on the CSs of layered crystals. The corresponding electron spectra of CSs weakly differ from the bulk ones [9, 13] and the "pattern" of the surface plane, i.e. its crystallography, reproduces the "pattern" of this plane in the bulk of layered crystal, in contrast to CSs for other semiconductors, e.g., crystalline Si [14]. In work [15], the absence of unsaturated electron bonds on the CS (0001) of a GaSe layered crystal was confirmed. The results of work [16] testify to the inertness of CS (0001) of MoS_2. At the same time, for chalcogenide layered crystals GaTe, the authors of work [17], using the LEED method, observed a partial reconstruction of CSs obtained under UHV from monoclinic to hexagonal.

In this work, we report the results of experimental LEED research concerning the stability of CS (100) of In_4Se_3 with respect to the atomic reconstruction in a wide temperature interval of 77–295 K. We also determined the thermal characteristics of surfaces such as the Debye temperature and the Debye–Waller factor. By studying the structure of diffraction reflexes and their temperature-induced shifts, we established the anisotropy of the thermal expansion of surfaces. Similar researches, as well as the obtained thermal characteristics of the CS (100) of In_4Se_3 obtained by us for the first time and reported in work [18], are important from the viewpoint of their application to the nanostructure fabrication.

A study of the thermodynamic characteristics for layered crystals of some chalcogenide compounds including In_4Se_3 was carried out in work [19]. Experimental researches of the Debye temperature in the crystals were carried out by measuring the heat ca-

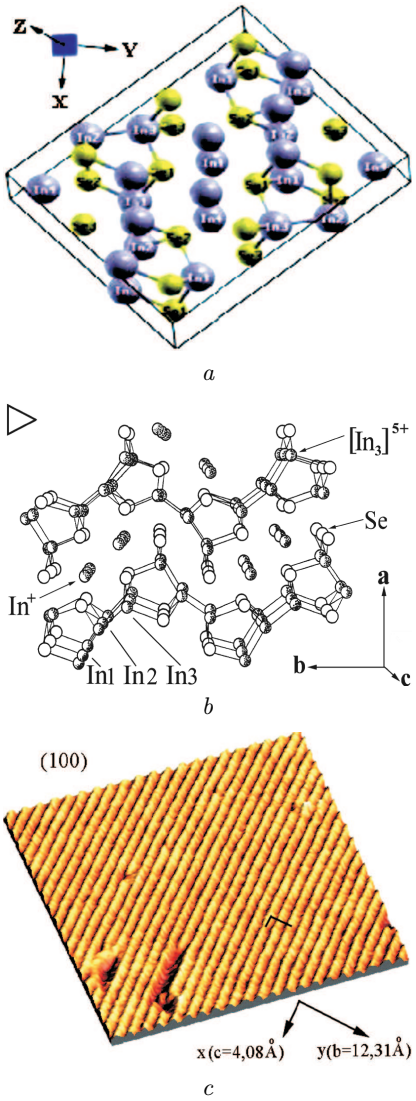

Fig. 1. Structural peculiarities of the In_4Se_3 layered crystal. (*a*) A unit cell of In_4Se_3 as the structure unit of the layer-packet. The axes X, Y, and Z are directed along the lattice vectors $\boldsymbol{c}$, $\boldsymbol{b}$, $\boldsymbol{a}$, respectively. The axes X and Y lie in the plane of CS (100). (*b*) Fragments of interlayer CSs (100) of In_4Se_3 according to the crystal structure (the projection on the plane (001)) illustrating which atoms are on the surface. The triangle in the left top corner shows the direction of cleaving. $[In_3]^{5+}$ is an indium polycation formed by covalently bonded In1, In2, and In3 indium atoms in the layer-packet. In^+ is an indium cation in the interlayer gap. (*c*) A fragment of 3D image of the STM pattern (a 36×36-nm^2 area) of the cleavage surface (100) of In_4Se_3 obtained under UHV and the chains along the x-direction (the lattice vector **c**). The STM pattern was obtained at a temperature of 80 K, a bias voltage of 2 V, and a tunnel current of 150 pA

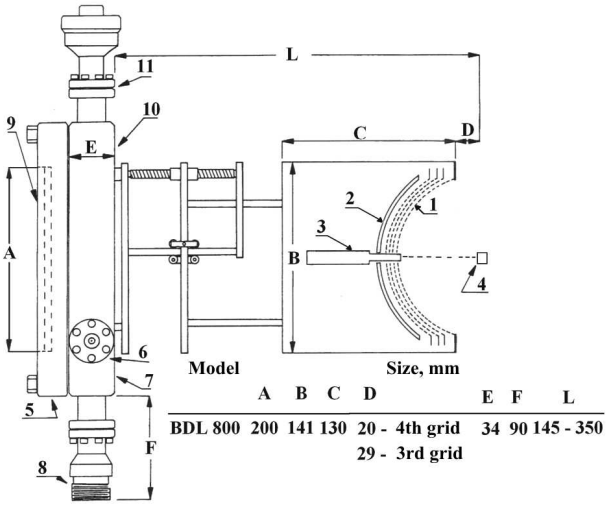

Fig. 2. Schematic diagram of the main units and details of the vacuum unit on the installation for LEED researches: (*1*) grids for the separation of electrons by their energy, (*2*) luminescent screen, (*3*) electron gun, (*4*) specimen, (*5*) flange with window 9 to observe LEED patterns from the specimen surface and record them with a digital video camera, (*6*) two vacuum feed-throughs symmetrically oriented at an angle of 54° with respect to the vertical axis, (*7*) flange for connecting the vacuum unit with a vacuum chamber, (*8*) entrance of electron gun power supply, (*9*) window, (*10*) UHV chamber, (*11*) vacuum feed-through for a regulator of the LEED experimental geometry

pacity in the low temperature interval. The data obtained were analyzed supposing that the main contribution to the heat capacity is given by phonons with the square-law dispersion. While discussing the results, we mark a probable influence of a feature in the phonon spectrum of layered structures – namely, the presence of a bend vibrational branch for the layer-packet regarded as a separate structural unit of layered crystals – on their thermodynamic characteristics. Therefore, we report two values, 192 and 73.7 K, for the Debye temperature in the bulk of In_4Se_3 layered crystal.

2. Experimental Technique. Results and Their Discussion

LEED experiments at energies of 25–72 eV were carried out on a BDL-800IR installation (OCI Vacuum Microengineering, http://www.ocivm.com) under a vacuum of 1.5×10^{10} Torr and in a temperature interval of 77–295 K. The vacuum unit of the installation was mounted on a header flange connected to the UHV chamber (see the schematic diagram in Fig. 2). For the crystallographic research of the atomically pure CS (100) of In_4Se_3 using the LEED method, specimens of a special form $3 \times 4 \times 6$ mm^3 in dimensions were cleaved *in situ* at 77 and 295 K with the help of an ultramicrotome knife fabricated of stainless steel.

Single-crystalline specimens of In_4Se_3 layered crystals grown up by the Czochralski method in a restored hydrogen atmosphere from the melt-solution of synthesized alloy In_4Se_3 + 10 at.% In with an over-stoichiometric In ($\leq$10 at.%) as a solvent were studied. In_4Se_3 layered crystals crystallized in the orthorhombic system and had a pronounced layered structure, whereas the layers had a complicated structure (Figs. 1, *a* and *b*) [5, 10]. In_4Se_3 crystals were characterized by rather a strong anisotropy of their physical properties, which should be directly reflected in the anisotropy and the features of properties for the CS (100) [10, 20, 21].

2.1. Structural features of In_4Se_3 layered crystals

The structural researches on a powder x-ray diffractometer Stoe STADI I showed that the orthorhombic phase corresponds to the structural formula In_4Se_3. In other words, the semiconductor layered crystal In_4Se_3 crystallized in the rhombic system and had an orthorhombic primitive lattice with the constants $\boldsymbol{a} = 15.296(1)$ Å, $\boldsymbol{b} = 12.308(1)$ Å, and $\boldsymbol{c} = 4.0806(4)$ Å, and the spatial group P_{nnm} (D_{2h}^{12}) [5–8, 10]. The fragments of its structure are depicted in Figs. 1, *a* and *b*.

Note that the In_4Se_3 layered crystal is not layered in the canonical meaning, i.e. it does not consist of plane layers coupled by the van der Waals interaction as, e.g., the layered crystals InSe and GaSe of the hexagonal system. Instead, it consists of nonplanar goffered layer-packets with weakened interlayer coupling. Therefore, the interlayer CSs (100) in In_4Se_3 also have the goffered structure (Figs. 1, *b* and *c*).

The three-dimensional image of a unit cell in the In_4Se_3 layered crystal obtained on the basis of structural researches is exhibited in Fig. 1, *a*. The interacting indium (In1, In2, In3) and selenium (Se) atoms in covalent-ionic bonds (Fig. 1, *b*), which belong to the same structural layer-packet, are connected with one another (except for In^+) and marked by chem-

ical element symbols. The axes XYZ describing the orientation of the unit cell are shown in the top of Fig. 1, *a*. Note that the bond anisotropy in the layers of layered crystals reveals itself in the anisotropy of their electron spectra [20, 21]. Such an illustration of a unit cell in the layered crystal allows one to take a better look at it to be convinced in the layered and chain goffered structure of interlayer CS (100) of In_4Se_3 obtained by the STM method [20] and depicted in Fig. 1, *b*. The illustration also testifies to the appearance of a dynamic disordering in the direction of the weak interlayer coupling [22].

The unit cell of In_4Se_3 includes 28 atoms grouped into two atomic monolayers and has seven crystallographically nonequivalent sites (4 with In and 3 with Se atoms); each of them occupies 4 equivalent positions (Figs. 1, *a* and *b*) and is in the following electronic configurations: $_{49}$In[Kr^{36} $4d^{10}$] $5s^2 5p^1$ and $_{34}$Se[Ar^{18} $3d^{10}$] $4s^2 4p^4$ with possible *sp*-hybridizations.

Note that, since the lattice in In_4Se_3 is orthorhombic, the reciprocal lattice is also orthorhombic, and the vectors of the direct and reciprocal lattices are antiparallel [23]. In Table 1, some structural information concerning the direct and reciprocal lattices in the In_4Se_3 crystal and the CS (100) is given. The constants of the orthorhombic lattice (space group $Pnnm$ (D_{2h}^{12})) were determined using the x-ray structural analysis.

It will be recalled that the LEED reflexes are interference maxima of plane de Broglie waves of electrons with the momentum $\mathbf{p} = \hbar\mathbf{k}$ ($\mathbf{k}$ is the electron wave vector) elastically and coherently scattered by the atoms on the surface. Therefore, the space of diffraction reflexes is a space of wave vectors or a space of the reciprocal lattice (the unit length is Å^{-1}), and the distances between the reflexes in certain directions are reciprocal lattice vectors (Fig. 3, left panel).

2.2. LEED at the atomically pure CS (100) of In_4Se_3 in the reflection geometry

LEED researches of In_4Se_3 layered crystals began in about 15–20 min after the crystals were cleaved under UHV ($P = 1.5\times10^{-10}$ Tott) at a temperature of 77 or 295 K. In the LEED unit (see Fig. 2), an electron gun with a filament cathode fabricated of a LaB_6 single crystal provided an electron beam current of 1–2 nA and a beam diameter of 0.25–1 mm in the plane of CS (100) of In_4Se_3 at energies of bombarding electrons of 25–72 eV. The beam intensity was enough for producing bright diffraction reflexes. LEED patterns were visualized with the use of a luminescent screen (Fig. 2) and recorded using a digital video camera. The analysis of the diffraction reflex intensities and the measurement of the distances between the reflexes were carried out with the help of the graphic software packages Gwyddion (http://gwyddion.net) and Adobe Photoshop (http://www.adobe.com).

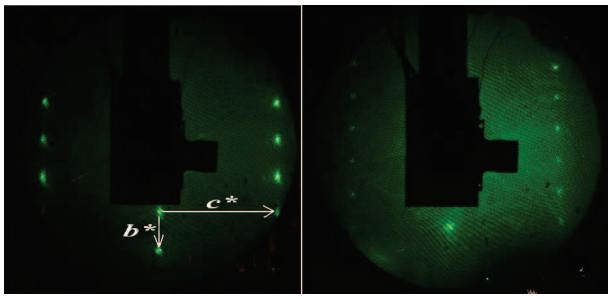

Fig. 3. LEED patterns (54 eV) obtained from the CSs (100) of In_4Se_3: just after cleaving *in situ* at a temperature of 77 K (left panel) and after the exposure for 12 h under UHV of 1.5×10^{-10} Torr(right panel). $\boldsymbol{b}^*$ and $\boldsymbol{c}^*$ are the reciprocal lattice vectors ($\boldsymbol{b}^* = 0.5104(7)$ Å and $\boldsymbol{c}^* = 1.5397(3)$ Å)

The orthorhombic character of the structure of semiconductor In_4Se_3 layered crystals and the local perfection of their CS (100) obtained *in situ* are testified by the LEED patterns depicted in Fig. 3. By the arrangement of diffraction reflexes, the patterns correspond to the surfaces of orthorhombic structures [1, 2]. The LEED patterns obtained for atomically pure CSs (100) of In_4Se_3 at an electron energy of 54 eV demonstrate the surface atomic structure (Fig. 3, the left and right panels) and evidence the perfection of CS (100) structure in the minimum coherence regions of the diffracting electron beam of about 0.1–1 μm.

Table 1. **Constants of three-dimensional direct and reciprocal (*) lattices in In_4Se_3**

$\boldsymbol{a}$, Å	$\boldsymbol{b}$, Å	$\boldsymbol{c}$, Å
15.296(1)	12.308(1)	4.0810(5)
$\boldsymbol{a}^*$, Å^{-1}	$\boldsymbol{b}^*$, Å^{-1}	$\boldsymbol{c}^*$, Å^{-1}
0.410(8)	0.510(4)	1.5397(4)

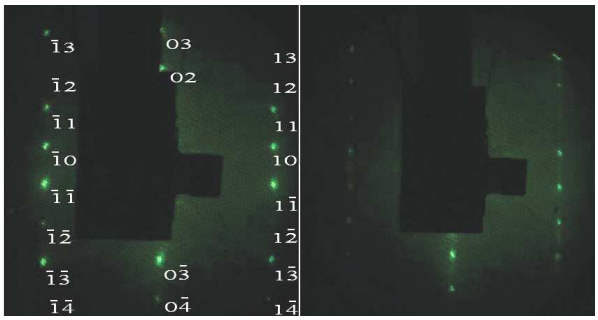

Fig. 4. LEED patterns (61 eV) obtained from the CSs (100) of In_4Se_3 at various temperatures of a specimen: 77 (left panel) and 295 K (right panel). Every reflex is marked by its indices, which correspond to the sites of the two-dimensional reciprocal lattice

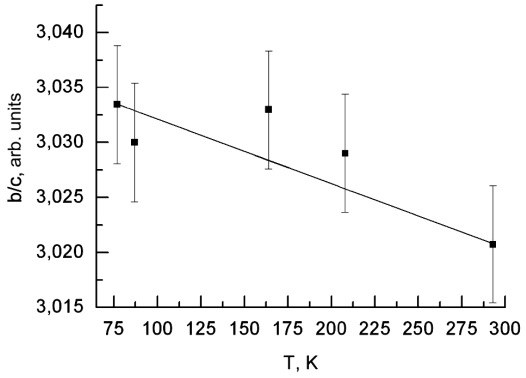

Fig. 5. Temperature dependence of the ratio between the lattice constants, b/c, for the CS (100) of In_4Se_3. The root-mean-square error bars are indicated

The exposure of CSs in the atmosphere of residual gases in the UHV chamber (10^{-10} Torr) for more than 10–12 h and, as a consequence, the formation of the interface coating on the surface by adsorbed gas molecules [10] resulted in a reduction of the diffraction reflex intensities and the smearing of the LEED pattern. However, the LEED pattern symmetry did not change (Fig. 3), which testified to the absence of atomic reconstruction in the monolayer-packet on the CS (100) of In_4Se_3 (see Figs. 1, *a* and *b*).

The LEED patterns for CSs (100) in In_4Se_3 obtained under UHV at various temperatures within the interval of 77–295 K showed that the specimen temperature growth resulted in the smearing of the LEED pattern, a reduction of the diffraction reflex intensities, and the growth of the background intensity. However, the symmetry of LEED patterns did not change (Fig. 4). This fact testifies to the thermal stability of atomically pure CSs (100) in In_4Se_3 and the absence of atomic reconstruction in the monolayer-packet on the CS (100).

The vectors in the left panel of Fig. 3 are compatible with the vectors $\boldsymbol{c}^*$ ($\boldsymbol{c}^* = 1.5397(3)$ Å^{-1}) and $\boldsymbol{b}^*$ ($\boldsymbol{b}^* = 0.510(3)$ Å^{-1}) of the two-dimensional reciprocal lattice on the CS (100) of In_4Se_3. The distances between the reflexes measured along the vectors $\boldsymbol{c}^*$ and $\boldsymbol{b}^*$ changed as the specimen temperature varied. In addition, the anisotropy in the linear expansion along the basis vectors $\boldsymbol{b}$ and $\boldsymbol{c}$ of the direct two-dimensional lattice on the CS (100) of In_4Se_3 was observed. One can see from Fig. 5 that the temperature coefficient of linear expansion along the lattice vector $\boldsymbol{c}$ is larger than that along the lattice vector $\boldsymbol{b}$. This fact was expectable on the basis of the anisotropy of electron spectra obtained for this surface in the $\boldsymbol{b}$- and $\boldsymbol{c}$-directions in works [20, 21]. In particular, for the $\boldsymbol{c}$ direction (along the In chains, Fig. 1, *b*), the obtained electron spectra $E(k_x)$ are typical of electrons that take part in the quasimetallic bonding.

It should be recalled that the ratios between the absolute values of two-dimensional reciprocal lattice vectors (the lattice constants) $\boldsymbol{c}^*/\boldsymbol{b}^*$ at various temperatures, which can be calculated from the LEED patterns registered for the CS (100) of In_4Se_3 at the corresponding temperatures, are equal to the ratios between the lattice constants of the direct lattice, $\boldsymbol{b}/\boldsymbol{c}$, which is illustrated in Fig. 5.

Note that the difficulties that arise while recording the LEED patterns with a pronounced brightness of diffraction reflexes from atomically clear CSs (100) of semiconductor In_4Se_3 layered crystals, especially at liquid-nitrogen temperatures, are associated with the low specific conductance of In_4Se_3. In particular, the specific conductance of undoped In_4Se_3 layered crystals equals $(1 \div 5) \times 10^{-2}$ $\Omega^{-1} \cdot \mathrm{cm}^{-1}$ at room temperature, but diminishes to $10^{-8} \div 10^{-10}$ $\Omega^{-1} \cdot \mathrm{cm}^{-1}$ as the temperature decreases to 77 K. The hindered draining of electrons from the bombarding beam can result in a local dynamic accumulation of the charge. The magnitude of this charge depends on the specimen thickness under the beam (2–3 mm), affects the energy of bombarding electrons, and can cause problems both in the record of the LEED patterns with a pronounced brightness of diffraction reflexes and with the background growth.

In Fig. 6, the intensity dependences of the diffraction reflexes with different coordinates in the LEED patterns on the energy of bombarding electrons within the interval of 25–72 eV are depicted. The corresponding wavelength interval for the incident and diffracting de Broglie electron waves ranges from 2.45 to 1.43 Å. The presented results testify to the most effective usage of electrons with energies of 47–65 eV in our experiments.

2.3. Debye temperature and Debye–Waller factor for CS(100) of In_4Se_3

Generally speaking, the Debye temperature is a parameter of a solid that determines the character of the temperature dependence of the heat capacity c_υ of the solid at a constant volume. The Debye temperature θ_D can be determined from the expression

$$k_\mathrm{B}\theta_\mathrm{D} = \hbar\omega_\mathrm{D}, \tag{1}$$

where k_B is the Boltzmann constant, $\hbar$ Planck's constant, and ω_D the maximum vibration frequency of acoustic phonons. Equation (1) means that the Debye temperature θ_D is a temperature of the crystal, at which the energy of the acoustic phonons of the lattice, $\hbar\omega_\mathrm{D}$, equals $k_\mathrm{B}\theta_\mathrm{D}$. The Debye temperature characterizes the stiffness of the lattice. It is higher for rigid lattices and lower for lattices with the soft type of elastic acoustic vibrations of atoms [24]. In the Debye theory, the crystalline solid is considered as an elastic continuum, in which the thermal vibrations are presented by a set of standing waves with frequencies ranging from $\omega = 0$ to $\omega = \omega_\mathrm{max}$. At temperatures $T \gg \theta_\mathrm{D}$, the temperature dependence of the heat capacity of solids at a constant volume approaches the classical Dulong–Petit law [24],

$$c_\upsilon = 3Nk_\mathrm{B} = 3R. \tag{2}$$

Whereas, at temperatures $T \gg \theta_\mathrm{D}$,

$$c_\upsilon = \frac{12\pi^4 Nk_\mathrm{B}T^3}{5\theta_\mathrm{D}^3} = 234Nk_\mathrm{B}\left(\frac{T}{\theta_\mathrm{D}}\right)^3, \tag{3}$$

where N is the number of atoms per unit cell volume in the crystal.

For the results of calculations of the Debye temperature and the Debye–Waller factor for the CS (100) of In_4Se_3 from the results of LEED measurements to be correct and the calculation errors to be minimum,

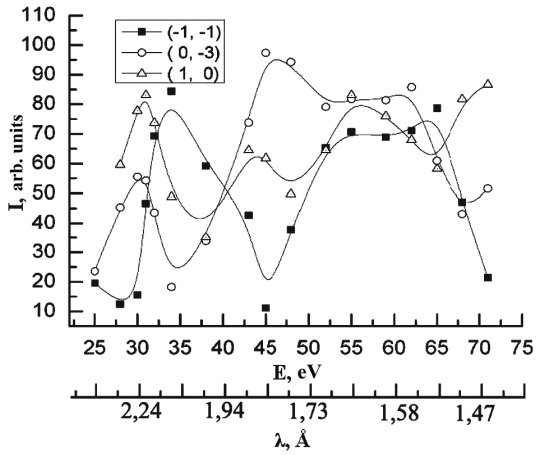

Fig. 6. Intensities of diffraction reflexes with different coordinates (see the left panel in Fig. 4) in the LEED patterns from the CS (100) of In_4Se_3 as functions of the bombarding electron energy (25–72 eV)

we selected those diffraction patterns, for which the intensities of diffraction reflexes were maximum. For this purpose, we studied the dependence of the LEED reflex intensities on the energy of bombarding electrons depicted in Fig. 6. The processing of reflexes and the estimation of their intensities were carried out using the graphic software packages Gwyddion and Adobe Photoshop.

For the LEED patterns with the symmetry indicated above (Figs. 3 and 4), which were recorded in the LEED experiments at various temperatures (Fig. 4) and where the intensity of reflexes decreased with the growth of the specimen temperature, we obtained that this behavior can be described by the following formula taken from works [24, 25]:

$$I\,(T) = I_0 \exp\left(-2W\left(\frac{T}{\theta_\mathrm{D}}\right)\right). \tag{4}$$

Here $I(T)$ is the intensity of a diffraction reflex at the specimen temperature T, I_0 the maximum intensity of a reflex observed at a temperature of 77 K and, accordingly, at the smallest vibration amplitude of surface atoms that scatter electron waves. The explicit expression for the coefficient $2W$ is [25]

$$2W = \frac{3T(\hbar\Delta k)^2}{2mk_\mathrm{B}\theta_\mathrm{D}^2}, \tag{5}$$

where W is the Debye–Waller factor, $\hbar\Delta k$ the momentum change of the electron at its scattering by

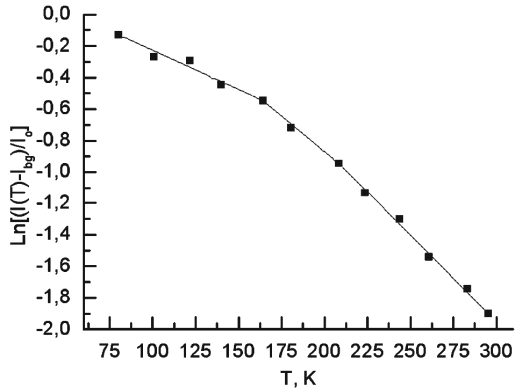

Fig. 7. Temperature dependence of the logarithm of the intensity I of a diffraction reflex $(\bar{1}, \bar{1})$ with regard for the background signal $I_{\rm bkgr}$ and with the normalization to its maximum value I_0 at 77 K

surface atoms, and m the averaged mass of a scattering center.

Owing to the known setup of LEED experiments in the reflection geometry for the observation of diffraction reflexes and the geometrical parameters of the LEED unit, the change of the electron momentum (wavevector) at the electron scattering by surface atoms can be expressed in the form [25, 26]

$$|\Delta\mathbf{k}| = |\mathbf{k}_f - \mathbf{k}_i| = \left|2k\cos\frac{\alpha}{2}\right|, \tag{6}$$

where α is the angle between the normal to the CS (100) of In_4Se_3 and the direction of the diffracted electron beam. According to the geometry of the LEED experiment, the angle α is small, and $\sin^2(\alpha/2)$ (the parallel component) is much less than $\cos^2(\alpha/2)$ (the normal component) [26].

The mass of a scattering center in Eq. (5) was calculated as the geometric mean

$$m = \sqrt{m_{\rm Se} m_{\rm In}} \tag{7}$$

of the Se and In atomic masses ($m_{\rm Se}$ and $m_{\rm In}$, respectively). The mass of selenium atom was calculated from the molar mass of selenium M(Se) and the Avogadro constant $N_{\rm A}$,

$$m_{\rm Se} = \frac{M\,({\rm Se})}{N_{\rm A}}. \tag{8}$$

The mass of an indium atom was determined analogously. As a result, the mass of a scattering center at the CS (100) of In_4Se_3 amounted to $m = 15.81 \times 10^{-26}$ kg.

We used Eq. (4), which describes the variation of the intensity of experimentally obtained diffraction reflexes in the interval of specimen temperatures from 77 to 295 K, in order to plot the temperature dependences of the logarithm of the intensity of primary brightest LEED reflexes $I(T)$. The background signal $I_{\rm bkgr}$ was subtracted, and the result was normalized by the maximum reflex intensity value obtained at 77 K,

$$\ln\left[\left(I\left(T\right) - I_{\rm bg}\right)/I_0\right] = f\left(T\right) = -2W =$$

$$= -\frac{3T\left(\hbar\Delta k\right)^2}{2mk_{\rm B}\theta_{\rm D}^2}, \tag{9}$$

Then, using Eqs. (5)–(9), we calculated the Debye temperature $\theta_{\rm D}$ and the Debye–Waller factor W for the CS (100) of In_4Se_3.

The intensities of diffraction reflexes from the CS (100) of In_4Se_3 were continuously registered with a digital video camera in the stepwise heating regime from 77 to 295 K and backward. The accuracy of current temperature measurements was ± 1 K. The following computer-assisted processing of the data and the estimation of the intensities of diffraction reflexes were carried out with the help of the graphic software packages indicated above.

In Fig. 7, the temperature dependence of the quantity $\ln\frac{I(T)-I_{\rm bkgr}}{I_0}$ (see the left-hand side of Eq. (9)) measured for the diffraction reflex $(\bar{1}, \bar{1})$ (see Fig. 4) in the temperature interval from 80 to 295 K with a step of about 20 K is depicted. The analysis of this dependence, as well as the analogous dependences for other bright reflexes – $(1, 0)$, $(1, \bar{1})$, $(\bar{1}, \bar{3})$, $(0, \bar{3})$, and $(1, 3)$ in the left panel of Fig. 4 – testifies that there exists three temperature intervals ($i = 1, 2, 3$), in which relationship (9) is obeyed, but with different "slopes" (see Table 2). On the basis of this fact, the thermal characteristics of the CSs (100) of In_4Se_3 – namely, the Debye temperature $\theta_{\rm D}^i$ and the Debye–Waller factor W^i – were calculated for each i-th interval. The effective values of the Debye temperature, $\theta_{\rm D}^{\rm eff}$, and the Debye–Waller factor, $W^{\rm eff}$, were evaluated as the geometric means of the corresponding $\theta_{\rm D}^i$- and W^i-values, respectively: $\theta_{\rm D}^{\rm eff}$=377 K (see Fig. 8) and $W^{\rm eff} = 0.00390$. Those values together with $\theta_{\rm D}^i$- and W^i-ones are quoted in Table 2.

Nevertheless, Fig. 8 demonstrates that the $W^{\rm eff}$-value (the dashed line) falls within the root-mean-

Table 2. **Results of calculations of the Debye temperature and the Debye–Waller factor for the CS (100) of In_4Se_3**

No.	Specimen temperature T, K	Temperature range, K	Debye temperature for the surface θ_D, K	Debye–Waller factor W, arb. units
1	122	80–164	398 ± 20	0.00240
2	186	164–208	358 ± 20	0.00451
3	251	208–295	377 ± 20	0.00549
Effective Debye temperature θ_D^{eff} and Debye–Waller factor W^{eff}			377 ± 20	0.00390

square error interval for each calculated θ_D^i-value, being identical to one of them ($\theta_D^{eff} = \theta_D^3 = 377$ K, see Table 2). In our opinion, this fact testifies that the Debye temperature is a temperature-independent quantity.

2.4. Estimation of the Debye temperature of In_4Se_3 crystal from the calculated phonon spectra

In order to evaluate the effective value of Debye temperature in the bulk of an In_4Se_3 layered crystal, formula (1) should be rewritten in the form

$$k_B\theta_D = \hbar\omega_{LA}^{max}, \tag{10}$$

where ω_{LA}^{max} is the maximum effective oscillation frequency of longitudinal acoustic phonons along the directions X, Y, and Z.

The dynamics of the lattice in an In_4Se_3 layered crystal was considered in work [27], where the corresponding phonon spectrum was calculated in the model of central pair interaction and making no allowance for long-range forces. The obtained phonon spectrum of the crystal contained a considerable number of low-frequency modes distorting, as the cited authors indicated, the "classical" form of acoustic branches. Therefore, the maximum effective frequency of longitudinal acoustic phonons, ω_{LA}^{max}, enters Eq. (10) and is required for the calculation of the effective Debye temperature in the bulk of the In_4Se_3 layered crystal, being taken as the geometrical mean of the maximum values $\omega_{LA}^{max}(k_x)$ in the X-direction, $\omega_{LA}^{max}(k_y)$ in the Y-direction, and $\omega_{LA}^{max}(k_z)$ in the Z-direction. According to the results of calculations by Eq. (10) and the data of work [27], the effective value of Debye temperature in the bulk of the In_4Se_3 layered crystal amounts to $\theta_D^{eff} = 132$ K. The same parameter evaluated by the same method, but for the plane of cleavage surface (XY), amounts to $\theta_D^{eff} = 108$ K.

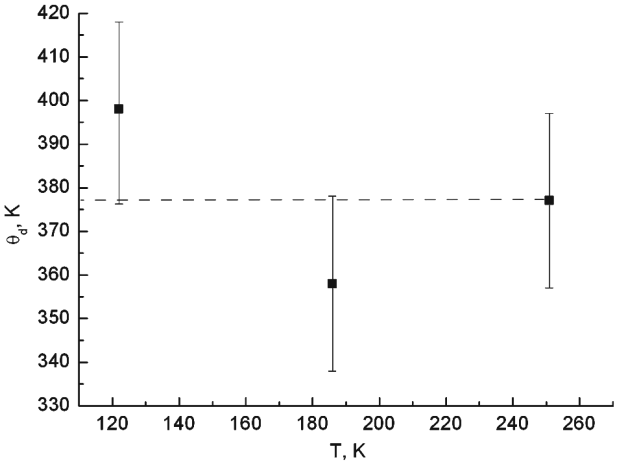

Fig. 8. "Temperature dependence" of the Debye temperature θ_D for the CSs (100) of In_4Se_3. The dashed line corresponds to the value of θ_D^{eff}. The root-mean-square error bars for θ_D^i ($i = 1, 2, 3,$) are indicated

This difference between the Debye temperatures for the CS (100) and the bulk of In_4Se_3 can be associated, first of all, with the difference between the dynamic constants describing the interaction between atoms, which, in turn, stems from different interaction symmetries on the surface and in the bulk [24]. It is also necessary to recall that, besides the existence of phonon spectra of a layer-packet [27], there also exist, as was shown in works [22, 28], special nonlinear bend vibrations of the layer-packet considered as a separate structural unit in the In_4Se_3 layered crystal. Those vibrations can change the effective value of Debye temperature for both bulk and CS (100) of In_4Se_3. Those manifestations of the dynamic disordering in the In_4Se_3 layered crystal in the direction of the weak van der Waals interlayer coupling and

the appearance of quasilocalized electron states in the electron energy structure was shown theoretically in works [22, 28]. Their geometrical localization on the CS (100) of In_4Se_3 was experimentally confirmed for the first time in our works [29, 30].

3. Conclusions

The structural researches of the CS (100) of In_4Se_3 layered crystals using the LEED method showed the following:

– The symmetry of the reciprocal lattice and the ratio $\boldsymbol{c}^*/\boldsymbol{b}^*$ between the lattice constants for the two-dimensional reciprocal lattices (and, respectively, the ratio $\boldsymbol{b}/\boldsymbol{c}$ between the lattice constants for the direct lattices) on the CS (100) of In_4Se_3 do not depend on the exposure time after the cleavage under UHV at a temperature of 295 K. This means that, after the cleavage, the lattice is not reconstructed, and the CS (100) of In_4Se_3 is structurally stable.

– The reduction of the intensity of diffraction reflexes obtained from the CS (100) of In_4Se_3 after a long exposure ($t_{\rm exp} > 10 \div 12$ h) under UHV and their certain smearing are associated with the formation of interfaces from the components of the atmosphere of residual gases in the UHV chamber.

The LEED patterns of atomically pure CS (100) of In_4Se_3 obtained under UHV at various temperatures showed that the growth of the specimen temperature results in the smearing of LEED patterns, the reduction of the intensities of diffraction reflexes, and the growth of the background signal. However, the symmetry of LEED patterns does not change. This fact testifies to the thermal stability of atomically pure CSs (100) of In_4Se_3 and the absence of atomic reconstruction in the monolayer-packet on the CS (100) of In_4Se_3.

The anisotropy of the linear expansion of the CS (100) of In_4Se_3 along the directions of lattice vectors $\boldsymbol{b}$ and $\boldsymbol{c}$ was established. The coefficient of temperature expansion along the vector $\boldsymbol{c}$ was found to be larger than the same coefficient along the vector $\boldsymbol{b}$.

The Debye temperature calculated for the CS (100) of In_4Se_3 from experimental data showed that it differs from the Debye temperature for the bulk of In_4Se_3. This fact can result from the existence of special nonlinear bend vibrations of the layer-packet as a separate structural unit of the In_4Se_3 layered crystal and a change in the symmetry of the interaction between atoms on the surface in comparison with the bulk. Together, those factors can affect the effective value of Debye temperature for the CS (100) of In_4Se_3 layered crystal.

1. K. Oura, V.G. Lifshits, A.A. Saranin, A.V. Zotov, and M. Katayama, *Surface Science. An Introduction* (Springer, Berlin, 2003).
2. D.P. Woodruff and T.A. Delchar, *Modern Techniques of Surface Science* (Cambridge University Press, Cambridge, 1994).
3. H. Wedler and K. Heinz, Vakuum Forsch. Prax. **2**, 107 (1995).
4. A.R. Shulman and S.A. Fridrikhov, *Secondary-Emission Methods for Investigations of Solids* (Nauka, Moscow, 1977) (in Russian).
5. U. Schwarz, H. Hillebrecht, H.J. Deiseroth, and R. Walther, Z. Kristallogr. **210**, 342 (1995).
6. P.V. Galiy, A.V. Musyanovych, and Ya.M. Fiyala, Physica E **35**, 88 (2006).
7. P.V. Galiy, T.M. Nenchuk, Ya.B. Losovyj, and Ya.M. Fiyala, Funct. Mater. **15**, 68 (2008).
8. P.V. Galiy, T.M. Nenchuk, O.R. Dveriy, A. Ciszewski, P. Mazur, and S. Zuber, Physica E **41**, 465 (2009).
9. W. Jaegermann, A. Klein, and C. Pettenkofer, in *Electron Spectroscopies Applied to Low-Dimensional Structures*, edited by H.I Hughes and H.P. Starnberg (Kluwer, Dordrecht, 2000), p. 317.
10. P.V. Galiy, T.M. Nenchuk, O.Ya. Melnyk, and Y.M. Stakhira, Ukr. Fiz. Zh. **48**, 256 (2003).
11. T.D. Henson, D. Sarid, and L.S. Bell, J. Microsc. **152**, 467 (1988).
12. J.M. Nicholls and J.M. Debever, Surf. Sci. **189/190**, 919 (1987).
13. J. Brandt, Dissert. zur Erlangung des Dokt. der Mathem.-Nat. (Kiel, 2003).
14. B.A. Nesterenko and V.G. Lyapin, *Phase Transitions on Free Faces and Phase Interfaces in Semiconductors* (Naukova Dumka, Kiev, 1990) (in Russian).
15. Li Ming, P. Thiry, and A. Degiovanni, Phys. Rev. B **49**, 11613 (1994).
16. Bo Ying Han, K. Hevesi, Yu. Li-Ming, J. Vacuum Sci. Technol. A **13**, 1036 (1994).
17. O.A. Balitskii, B. Jaeckel, and W. Jaegermann, Phys. Lett. A **372**, 3303 (2008).
18. P.V. Galiy, Ya.B. Losovyj, T.M. Nenchuk, and I.R. Yarovets, in *Abstracts of the 6th International Workshop on Surface Physics, 1–6 September 2013, Niemcza, Poland* (University of Wroclaw, Wroclaw, 2013), p. 51.
19. E.E. Anders, B.Ya. Sukharevskii, and L.S. Shestachenko, Fiz. Nizk. Temp. **5**, 783 (1979).
20. Ya.B. Losovyj, M. Klinke, E. Cai, I. Rodriges, J. Zhang, L. Makinistian, A.G. Petukhov, E.A. Albanesi, P. Galiy,

Ya. Fiyala, J. Liu, and P.A. Dowben, Appl. Phys. Lett. **92**, 122107 (2008).
21. Ya.B. Losovyj, L. Makinistian, E. Albanesi, A.G. Petukhov, J. Liu, P.V. Galiy, O.R. Dveriy, and P.A. Dowben, J. Appl. Phys. **104**, 083713 (2008).
22. I.M. Stakhira and P.G. Ksyondzyk, Ukr. Fiz. Zh. **26**, 762 (1981).
23. B.F. Ormont, *Introduction to Physical Chemistry and Crystal Chemistry of Semiconductors* (Vysshaya Shkola, Moscow, 1973) (in Russian).
24. J.W. Niemantsverdriet, *Spectroscopy in Catalysis. An Introduction* (Wiley, Weinheim, 2007).
25. C.N. Borca, T. Komesu, H.-k. Jeong, P.A. Dowben, and D. Ristoiu, Appl. Phys. Lett. **77**, 88 (2000).
26. K. Fukutani, N. Lozova, S.M. Zuber, P.A. Dowben, P.V. Galiy, and Ya.B. Losovyj, Appl. Surf. Sci. **256**, 4796 (2010).
27. D.M. Bercha and K.Z. Rushchanskii, Fiz. Tverd. Tela **40**, 2103 (1998).
28. I.M. Stakhira and P.G. Ksyondzyk, Ukr. Fiz. Zh. **27**, 1186 (1982).
29. P.V. Galiy, T.M. Nenchuk, V.P. Savchin, and Y.M. Stakhira, Ukr. Fiz. Zh. **40**, 230 (1995).
30. P.V. Galiy, T.M. Nenchuk, and J.M. Stakhira, J. Phys. D **34**, 18 (2001).

Received 02.08.13.
Translated from Ukrainian by O.I. Voitenko

П.В. Галій, Я.Б. Лозовий, Т.М. Ненчук, І.Р. Яровець

СТРУКТУРНІ ДОСЛІДЖЕННЯ ПОВЕРХОНЬ СКОЛЮВАННЯ (100) ШАРУВАТИХ КРИСТАЛІВ In_4Se_3 МЕТОДОМ ДИФРАКЦІЇ ПОВІЛЬНИХ ЕЛЕКТРОНІВ

Р е з ю м е

Методом дифракції повільних електронів на відбивання досліджено стабільність структури поверхонь сколювання (100) шаруватих кристалів In_4Se_3 та їх "теплові" характеристики. Показано, що поверхні сколювання (100) In_4Se_3 є структурно стабільними, і не зазнають атомної реконструкції у широкому температурному діапазоні 77–295 K. За результатами експериментів з температурної залежності інтенсивності дифракційних рефлексів, яка зменшується з ростом температури зразка, одержано такі теплові характеристики поверхонь сколювання, як: температура Дебая та фактор Дебая–Уоллера. Розрахована температура Дебая поверхонь сколювання (100) In_4Se_3 є температурнозалежною величиною, і її значення є різними у трьох різних температурних областях для вказаного вище температурного діапазону 77–295 K. Підтверджено, що температура Дебая для поверхонь сколювання (100) In_4Se_3 та для об'єму кристала є різною, а також встановлено анізотропію теплового розширення поверхонь сколювання за основними кристалографічними напрямками у площині сколу (100) In_4Se_3.